SCIENTIFIC REPORTS

OPEN

SUBJECT AREAS:
QUANTUM INFORMATION
NONLINEAR OPTICS
SUPERCONDUCTING DEVICES
SINGLE PHOTONS AND QUANTUM EFFECTS

Received
30 July 2014

Accepted
7 November 2014

Published
9 December 2014

Correspondence and requests for materials should be addressed to Y.-X.L. (yuxiliu@mail.tsinghua.edu.cn)

Controllable microwave three-wave mixing via a single three-level superconducting quantum circuit

Yu-xi Liu[1,2,3], Hui-Chen Sun[1,3], Z. H. Peng[3], Adam Miranowicz[3,4], J. S. Tsai[3,5] & Franco Nori[3,6]

[1]Institute of Microelectronics, Tsinghua University, Beijing 100084, China, [2]Tsinghua National Laboratory for Information Science and Technology (TNList), Beijing 100084, China, [3]CEMS, RIKEN, Saitama 351-0198, Japan, [4]Faculty of Physics, Adam Mickiewicz University, 61-614 Poznań, Poland, [5]NEC Green Innovation Research Laboratories, Tsukuba, Ibaraki 305-8501, Japan, [6]Physics Department, The University of Michigan, Ann Arbor, Michigan 48109-1040, USA.

Three-wave mixing in second-order nonlinear optical processes cannot occur in atomic systems due to the electric-dipole selection rules. In contrast, we demonstrate that second-order nonlinear processes can occur in a superconducting quantum circuit (i.e., a superconducting artificial atom) when the inversion symmetry of the potential energy is broken by simply changing the applied magnetic flux. In particular, we show that difference- and sum-frequencies (and second harmonics) can be generated in the microwave regime in a controllable manner by using a single three-level superconducting flux quantum circuit (SFQC). For our proposed parameters, the frequency tunability of this circuit can be achieved in the range of about 17 GHz for the sum-frequency generation, and around 42 GHz (or 26 GHz) for the difference-frequency generation. Our proposal provides a simple method to generate second-order nonlinear processes within current experimental parameters of SFQCs.

Nonlinear optical effects have many fundamental applications in quantum electronics, atom optics, spectroscopy, signal processing, communication, chemistry, medicine, and even criminology. These phenomena include optical Raman scattering, frequency conversion, parametric amplification, the Pockels and Kerr effects (i.e., linear and nonlinear electro-optical effects), optical bistability, phase conjugation, and optical solitons[1,2]. Three-wave mixing (including the generations of the sum-frequency, difference-frequency, and second harmonics) and four-wave mixing are important methods to study nonlinear optics. It is well-known that materials without inversion symmetry can exhibit both second- and third-order nonlinearities. However, materials with inversion symmetry usually exhibit only third-order nonlinearities. Thus, three-wave mixing (which requires the second-order nonlinearity) cannot occur in atomic systems with well-defined inversion symmetry, because the electric-dipole transition selection rules produce a zero signal[1] with mixed frequencies. Although chiral molecular three-level systems without inversion symmetry can be used to generate three-wave mixing in the microwave domain[3–6], such wave mixing cannot be tuned because the energy structure of the systems is fixed by nature.

Recently, superconducting charge, flux, and phase quantum circuits based on Josephson junctions have been extensively explored as basic building blocks for solid-state quantum information processing[7–10]. These circuits can also be considered as artificial atoms[9,11]. In contrast to natural atoms, the quantum energy structure and the potential energy of these artificial atoms can usually be tuned by external parameters. Thus, they can possess new features and can be used to demonstrate fundamentally new phenomena which cannot be found in natural three-level atoms. For example, with the tunable potential energy of superconducting flux quantum circuits (SFQCs) by varying the bias magnetic flux, three-level (qutrit) SFQCs can have a Δ-type (cyclic) transition[12]. Two-level SFQCs are also known as superconducting flux qubits[13]. Three-level SFQCs (i.e., superconducting flux qutrits) can be used to demonstrate the coexistence of single- and two-photons[12,14], which does not occur in natural three-level atomic systems with electric-dipole interaction. Such Δ-type atoms can also be used to cool quantum systems[15], or generate microwave single-photons[16].

In solid-state quantum information processing, microwave signals are usually employed for measuring and controlling the qubits. Moreover, these signals can also be used to detect the motion of nanomechanical resonators[17] and to read out the spin information in nitrogen-vacancy centers in diamonds[18]. Therefore, the controllable generation, conversion and amplification of microwave signals play a very important role in solid-state

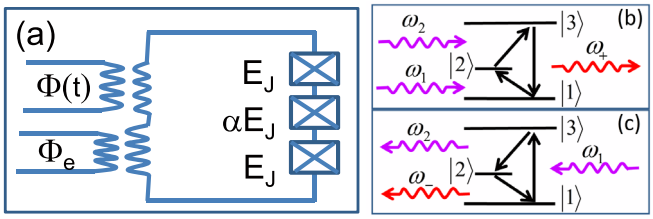

Figure 1 | (a) Schematic diagram for a SFQC with three Josephson junctions biased by a magnetic flux Φ_e and also driven by the magnetic flux $\Phi(t)=\sum_l \Phi(\omega_l)\exp(-i\omega_l t)$ with different frequencies ω_l, which are specified in panels (b,c); E_J is the Josephson energy, and $0.5<\alpha<1$. (b) A three-level (qutrit) SFQC, which can be considered as an artificial atom with Δ-type (cyclic) transitions driven by the external magnetic flux $\Phi(\omega_1)$ [$\Phi(\omega_2)$] with frequency ω_1 (ω_2) to induce the transition between the energy levels $|1\rangle$ and $|2\rangle$ ($|2\rangle$ and $|3\rangle$), results in the generation of the output signal with the sum-frequency ω_+; (c) Same as in panel (b) but for the flux $\Phi(\omega_1)$ inducing the transition between the energy levels $|1\rangle$ and $|3\rangle$, leads to the generation of the output signal with the difference-frequency ω_-.

quantum information processing. The generation of microwave Fock's states[19–21], superpositions of different Fock's states[22], squeezed states[23], nonclassical microwave[24] and giant Kerr nonlinearities[25,26] have been studied in the microwave domain via circuit quantum electrodynamics (QED)[7–9]. Microwave parametric amplification[27] has also been studied by using three-wave mixing[28] in superconducting circuits with four Josephson junctions. Different from Ref. 28, here we propose another method to generate microwave three-wave mixing, including the generation of the sum- and difference-frequencies in a controllable way via a tunable single SFQC. This method also applies for phase[29–31] and transmon[32] qutrits. In our proposal, such three-wave mixing can be switched off at the optimal point by the bias magnetic flux. We also discuss the possibility for the generations of second harmonics and zero-frequency using SFQCs.

Model

To be specific, our study below will focus on three-level SFQCs, also called a qutrit or three-level qudit. However, our results can also be applied to phase and transmon qutrits. As shown in Fig. 1(a), a SFQC consists of a superconducting loop interrupted by three Josephson junctions and controlled by a bias magnetic flux Φ_e. The Josephson energies (capacitances) of the two identical junctions and the smaller one are E_J (C_J) and αE_J (αC_J) with $0.5<\alpha<1$, respectively. If we assume that the SFQC is driven by the external time-dependent magnetic flux $\Phi(t)=\sum_l \Phi(\omega_l)\exp(-i\omega_l t)$ with frequencies ω_l, then we can describe the system by this Hamiltonian

$$H=-\frac{\hbar^2}{2M_p}\frac{\partial^2}{\partial\varphi_p^2}-\frac{\hbar^2}{2M_m}\frac{\partial^2}{\partial\psi_m^2}+U\left(\varphi_p,\varphi_m,f\right)+V(t) \quad (1)$$

with $M_p=2C_J[\Phi_0/(2\pi)]^2$ and $M_m=M_p(1+2\alpha)$. The potential energy is

$$U\left(\varphi_p,\varphi_m,f\right)=2E_J\left(1-\cos\varphi_p\cos\varphi_m\right)+\alpha E_J[1-\cos(2\pi f+2\varphi_m)], \quad (2)$$

with phases $\varphi_p=(\phi_1+\phi_2)/2$ and

$$\varphi_m=\frac{1}{2}(\phi_2-\phi_1)+\frac{2\pi\alpha}{2\alpha+1}\frac{\Phi(t)}{\Phi_0}, \quad (3)$$

where ϕ_1 and ϕ_2 are the gauge-invariant phases of the two identical junctions (see Fig. 1). Here $f=\Phi_e/\Phi_0$ is the reduced magnetic flux, and $\Phi_0=h/(2e)$ is the flux quantum. The interaction between the SFQC and the time-dependent magnetic flux is described by $V(t)=I(\varphi_p,\varphi_m,f)\Phi(t)$, with the supercurrent

$$I\left(\varphi_p,\varphi_m,f\right)=\frac{\alpha I_0}{2\alpha+1}\left[\sin(2\pi f+2\varphi_m)-2\sin\varphi_m\cos\varphi_p\right] \quad (4)$$

inside the superconducting loop[33,34] and $I_0=2\pi E_J/\Phi_0$. The supercurrent $I\equiv I(\varphi_p,\varphi_m,f)$ and the external magnetic flux $\Phi(t)$ are equivalent to the electric dipole moment operator and time-dependent electric field of the electric dipole interaction in atomic systems. It is obvious that $U(\varphi_p,\varphi_m,f)$ in Eq. (1) can be tuned by the bias magnetic flux Φ_e. We have shown that one of two flux quits cannot work at the optimal point when both qubits are directly coupled through their mutual inductance[34], because of its selection rules[12,33]. Such problem can be solved by introducing a coupler (e.g., see, Refs. 35–37).

We have shown[12] that three-level SFQCs have Δ-type (cyclic) transitions among the three lowest energy levels $|i\rangle$ when the inversion symmetry of the potential energy is broken, otherwise it has a cascade transition. Under the three-level approximation of SFQCs, Eq. (1) becomes

$$H_T=\sum_{i=1}^{3}E_i|i\rangle\langle i|+V_T(t), \quad (5)$$

where E_i ($i=1,2,3$) are three eigenvalues corresponding to the three lowest eigenstates $|i\rangle$ of Eq. (1) with $V(t)=0$. With this three-level approximation of SFQCs, the interaction Hamiltonian $V_T(t)$ in Eq. (5) can be generally written as

$$V_T(t)=\left[\sum_{i,j=1,i<j}^{3}I_{ij}(f)\sigma_{ij}+\text{H.c.}\right]\Phi(t), \quad (6)$$

with operators $\sigma_{ij}=|i\rangle\langle j|$ and matrix elements $I_{ij}(f)\equiv\langle i|I(\varphi_p,\varphi_m,f)|j\rangle$ dipole-like moment operator. Here, the longitudinal coupling $\sum_{i=1}^{3}I_{ii}(f)\sigma_{ii}\Phi(t)$ between the three-level SFQC and the time-dependent magnetic flux is neglected even though the reduced magnetic flux is not at the optimal point, i.e., $f\neq 0.5$. We note that $f=0.5$ is called as the optimal point or the symmetry point[13], where the influence of flux noise is minimal. When the relaxation and dephasing of the three-level SFQC are included, the dynamics can be described by the master equation

$$\dot{\rho}(t)=\frac{1}{i\hbar}[H_T,\rho]+\frac{1}{2}\sum_{i=2}^{3}\gamma_{ii}(2\sigma_{ii}\rho\sigma_{ii}-\sigma_{ii}\rho-\rho\sigma_{ii}-\bar{\rho}_{ii})-\frac{1}{2}\sum_{l=1}^{3}\sum_{i<j}\gamma_{ij}\left[\left(\sigma_{jj}\rho-\bar{\rho}_{jl}\sigma_{jl}\right)-\left(\rho\sigma_{jj}-\bar{\rho}_{lj}\sigma_{lj}\right)\right]+\sum_{i<j}\gamma_{ij}\sigma_{ij}\left(\rho-\bar{\rho}_{jj}\right)\sigma_{ji}, \quad (7)$$

with $\rho(t)\equiv\rho$. Here, different energy levels are assumed to have different dissipation channels. The operator $\rho(t)$ is the reduced density matrix of the three-level SFQC. We will study the steady-state response; thus, the thermal equilibrium state $\bar{\rho}$ for $V(t)=0$ with matrix elements $\bar{\rho}_{lj}$ is added to the master equation. Also, γ_{ii} is the pure dephasing rate of the energy level $|i\rangle$, while $\gamma_{ij}=\gamma_{ji}$ (with $i\neq j$) are the off-diagonal decay rates.

Sum- and difference-frequency generations

We assume that the SFQC is in the thermal equilibrium state $\bar{\rho}$ when $V(t)=0$. To study the steady-state response of the three-level SFQC to weak external fields, we have to obtain the solution of the reduced density matrix ρ for the three-level SFQC in Eq. (7) by solving the following equations:

$$\begin{aligned}
\dot{\rho}_{ij}(t) &= \frac{1}{i\hbar}[H_T,\rho(t)]_{ij} - \frac{1}{2}\Gamma_{ij}\tilde{\rho}_{ij}(t),\ i\neq j,\\
\dot{\rho}_{11}(t) &= \frac{1}{i\hbar}[H_T,\rho(t)]_{11} + \gamma_{12}\tilde{\rho}_{22}(t) + \gamma_{13}\tilde{\rho}_{33}(t),\\
\dot{\rho}_{22}(t) &= \frac{1}{i\hbar}[H_T,\rho(t)]_{22} - \gamma_{12}\tilde{\rho}_{22}(t) + \gamma_{23}\tilde{\rho}_{33}(t),\\
\dot{\rho}_{33}(t) &= \frac{1}{i\hbar}[H_T,\rho(t)]_{33} - (\gamma_{13}+\gamma_{23})\tilde{\rho}_{23}(t)
\end{aligned} \tag{8}$$

with the parameters $\Gamma_{12} = \gamma_{12}$, $\Gamma_{13} = \gamma_{13} + \gamma_{23} + \gamma_{33}$ and $\Gamma_{23} = \gamma_{12} + \gamma_{13} + \gamma_{23} + \gamma_{22} + \gamma_{33}$, derived from Eq. (7). Note that $\Gamma_{ij} = \Gamma_{ji}$. Here we define $\tilde{\rho}_{ij}(t) = \rho_{ij}(t) - \bar{\rho}_{ij}$. Because the external fields are weak, the solution of $\rho(t)$ can be obtained by expressing $\rho(t)$ in the form of a perturbation series in $V_T(t)$, i.e.,

$$\rho(t) = \rho_0 + \rho_1(t) + \rho_2(t) + \cdots, \tag{9}$$

with the density matrix operator $\rho_0 = \bar{\rho}$ in the zeroth-order approximation. We define the magnetic polarization P due to the external field as $P = \mathrm{Tr}[\rho(t)I]$, in analogy to the electric polarization[1], then the second-order magnetic polarization can be given as $P^{(2)} = \mathrm{Tr}[\rho_2(t)I]$, and then the second-order magnetic susceptibility can be given by

$$\chi^{(2)}(\omega) = \frac{P^{(2)}(\omega)}{\Phi(\omega_1)\Phi(\omega_2)}. \tag{10}$$

In our study, since the condition $|E_i - E_j| \gg k_B T$ (with $i \neq j$) is satisfied, then the system is in its ground state $|1\rangle$ in the thermal equilibrium state, i.e., $\rho_0 = \bar{\rho} = |1\rangle\langle 1|$.

Sum-frequency generation. To study the microwave generation of the sum-frequency, we now assume that the two external magnetic fluxes are applied to the three-level SFQC. As schematically shown in Fig. 1(b), one magnetic flux with frequency ω_1 (ω_2) induces the transition between the energy levels $|1\rangle$ and $|2\rangle$ ($|2\rangle$ and $|3\rangle$). In this case, the interaction Hamiltonian $V_T(t)$ between the three-level SFQC and the two external fields is given by

$$V_1(t) = \sum_{i=1,2} I_{i,i+1}(f)\sigma_{i,i+1}\Phi(\omega_i)\exp(\mathrm{i}\omega_i t) + \mathrm{H.c.} \tag{11}$$

under the rotating-wave approximation. On replacing $V_T(t)$ in Eq. (7) by $V_1(t)$, and using the perturbation theory discussed above, we can obtain the reduced density matrix of the three-level SFQC, up to second order in $V_1(t)$, and find the second-order magnetic susceptibility as

$$\chi^{(2)}(\omega_+) = \frac{I_{12}(f)I_{23}(f)I_{31}(f)}{(\mathrm{i}\omega_1 - \mathrm{i}\omega_{21} + \Gamma_{21})(\mathrm{i}\omega_+ - \mathrm{i}\omega_{31} + \Gamma_{31})} \tag{12}$$

for the sum-frequency generation with $\omega_+ = \omega_1 + \omega_2$, and $\omega_{ij} = (E_i - E_j)/\hbar$, with $i > j$. Equation (12) obviously shows that the second-order magnetic susceptibility is proportional to the product of the three different electric dipole-like matrix elements (or transition matrix elements) $I_{ij}(f)$, with $i \neq j$. Therefore, for a given reduced magnetic flux f, the maximum value of the susceptibility in Eq. (12) is $\chi^{(2)}_{\max}(\omega_+) = I_{12}I_{23}I_{31}/(\Gamma_{21}\Gamma_{31})$ when $\omega_+ = \omega_{31}$ and $\omega_1 = \omega_{21}$.

Difference-frequency generation. Similarly, the difference-frequency can also be generated by using a three-level SFQC. We assume that a magnetic flux with frequency ω_1 (ω_2) is applied between the energy levels $|1\rangle$ and $|3\rangle$ ($|2\rangle$ and $|3\rangle$) as shown in Fig. 1(c). In this case, the interaction between the three-level SFQC and the external magnetic fields can be described by

$$V_2(t) = \sum_{i=1,2} I_{i,3}(f)\sigma_{i,3}\Phi(\omega_i)\exp(\mathrm{i}\omega_i t) + \mathrm{H.c.} \tag{13}$$

under the rotating-wave approximation.

Using the same calculation as for Eq. (12), we can also obtain the second-order magnetic susceptibility of the difference-frequency $\omega_- = \omega_2 - \omega_1$ as

$$\chi^{(2)}(\omega_-) = \frac{I_{13}(f)I_{21}(f)I_{32}(f)}{(\mathrm{i}\omega_- - \mathrm{i}\omega_{21} + \Gamma_{21})(\mathrm{i}\omega_1 - \mathrm{i}\omega_{31} + \Gamma_{31})}. \tag{14}$$

For a given reduced magnetic flux f, the maximum amplitude $\chi^{(2)}_{\max}(\omega_-) = I_{13}I_{21}I_{32}/(\Gamma_{21}\Gamma_{31})$ of the susceptibility in Eq. (14) for the difference-frequency can be obtained under the resonant driving conditions: $\omega_- = \omega_{21}$ and $\omega_1 = \omega_{31}$.

Numerical simulation. Both Eqs. (12) and (14) show that the susceptibilities of the sum- and difference-frequencies can be controlled by the bias magnetic flux Φ_e. According to the analysis of the inversion symmetry for flux quantum circuits[12], we know that the three-level SFQC has a well-defined symmetry at the optimal point $f = 0.5$ and it behaves as natural three-level atoms with the Ξ-type (or ladder-type) transition. In this case, the transition matrix elements between the energy levels $|1\rangle$ and $|3\rangle$ is zero, i.e., $I_{13}(f = 0.5) = I_{31}(f = 0.5) = 0$, and both susceptibilities, $\chi^{(2)}(\omega_+)$ in Eq. (12) and $\chi^{(2)}(\omega_-)$ in Eq. (14), are zero. Thus, the microwave sum- or difference-frequencies cannot be generated at the optimal point as for natural three-level atoms with the electric-dipole selection rule. Equations (12) and (14) also tell us that the amplitudes of the susceptibilities for both the sum- and difference-frequencies are proportional to the modulus $R(f)$ of the product of the three different transition matrix elements, i.e.,

$$R(f) \equiv |I_{12}(f)I_{23}(f)I_{31}(f)| = |I_{21}(f)I_{32}(f)I_{13}(f)|. \tag{15}$$

Thus, the maximum value $R^{(\max)}(f)$ of $R(f)$ corresponds to the maximal susceptibilities under the resonant driving condition. To show clearly how the bias magnetic flux Φ_e can be used to control the sum- and difference-frequency generations, the three transition elements $|I_{12}|$, $|I_{23}|$ and $|I_{13}|$ versus the reduced magnetic flux f are plotted in Fig. 2(a). Also, the f-dependent product $|I_{12}I_{23}I_{31}|$ is plotted in Fig. 2(b). Here, we take experimentally accessible parameters, for example, $\alpha = 0.8$, $E_J/h = 192$ GHz, and $E_J/E_c = 48$, where E_c is the charging energy and h is the Planck constant. These data are taken from the RIKEN-NEC group for their most recent, unpublished, experimental setup. Figures 2(a) and 2(b) clearly show that the bias magnetic flux Φ. i.e., $f = \Phi/\Phi_0$, can be used to tune the transition elements, and then $R(f)$ is also tunable. We find that $R(f)$ is zero, at the optimal point corresponding to the zero signal for the sum- and difference-frequency generations, because the transition selection rule at this point makes the transition element $I_{13} = 0$, as shown in Fig. 2(a). That is, the transition between the energy levels $|1\rangle$ and $|3\rangle$ is forbidden. However, the sum- and difference-frequencies can be generated when $f \neq 0.5$, and the maximum $R^{(\max)}(f)$ corresponds to two symmetric points with $f = 0.4992$ and $f = 0.5008$. To show the tunability of the frequency generation, we now define a maximum variation $\delta_{ij}^{(\max)}(i > j)$ of the sum- and difference-frequency generation as

$$\delta_{ij}^{(\max)} = \frac{1}{2\pi}\left(\omega_{ij} - \omega_{ij}^{(\mathrm{opt})}\right) \tag{16}$$

for a given range of the reduced magnetic flux f. Here, $\omega_{ij}^{(\mathrm{opt})}$ denotes the transition frequency between the energy levels $|i\rangle$ and $|j\rangle$ at the optimal point.

Figure 2(c) shows that the maximum variation $\delta_{31}^{(\max)}$ of the sum-frequency is $\delta_{31}^{(\max)} = \left(\omega_{31} - \omega_{31}^{(\mathrm{opt})}\right)/(2\pi) \approx 17$ GHz for $0.5 < f <$

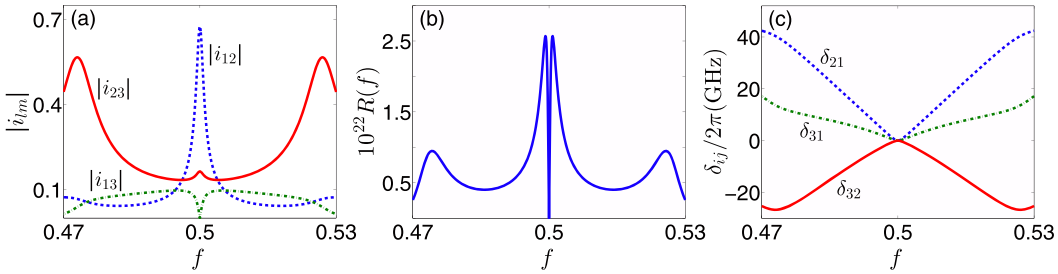

Figure 2 | (a) Modulus of the renormalized transition elements $i_{12} = I_{12}/I_0$, $i_{23} = I_{23}/I_0$, and $i_{13} = I_{13}/I_0$ versus the reduced magnetic flux f. The modulus $R(f)$, given by Eq. (15), and the detuning $\delta_{ij}(f) = \omega_{ij}(f) - \omega_{ij}^{(\mathrm{opt})}$, versus f, are plotted in panels (b) and (c), respectively. Here, $\omega_{ij}(f)$ $\left(\omega_{ij}^{(\mathrm{opt})}\right)$ are the f-dependent transition frequencies (transition frequencies at the optimal point with $f = 0.5$) between two different energy levels $|i\rangle$ and $|j\rangle$ $(i > j)$. The SFQC parameters are here taken as $E_J/h = 192$ GHz, $E_J/E_c = 48$, and $\alpha = 0.8$ with h being the Planck constant.

0.53. However, the maximum variation $\delta_{21}^{(\max)}$ or $\delta_{32}^{(\max)}$ of the difference-frequency is $\delta_{21}^{(\max)} = \left(\omega_{21} - \omega_{21}^{(\mathrm{opt})}\right)/(2\pi) \approx 42$ GHz or $\delta_{32}^{(\max)} = \left(\omega_{32} - \omega_{32}^{(\mathrm{opt})}\right)/(2\pi) \approx 26$ GHz for $0.5 < f < 0.53$. Thus, the tunability for the sum- and difference-frequency generations can be, in principle, over a very wide GHz range, by using the bias magnetic flux Φ_e.

Second-harmonic generation

From Eqs. (12) and (14), we find that the second-harmonic and zero-frequency signals can also be generated in three-level SFQCs when two applied external fields have the same frequency and satisfy the condition

$$\omega_1 = \omega_2 = \frac{1}{2}\omega_{31} = \bar{\omega}. \tag{17}$$

Let us now discuss second-harmonic generation. As shown in Fig. 3(a), we can find two values of the reduced magnetic flux, $f = 0.4878$ or $f = 0.5122$, such that $\omega_{31} = 2\omega_{21} = 2\omega_{32}$. In this case, the susceptibility of the second harmonic reaches its maximum, when an external field with the same frequency as $\omega_{21} = \omega_{32}$ is applied to the three-level SFQC. However, the second-order susceptibility becomes small when the magnetic field deviates from the points $f = 0.4878$ or $f = 0.5122$ because of the anharmonicity of the energy-level structure for the SFQC. If we assume that the anharmonicity is characterized by

$$\delta(f) = \bar{\omega}(f) - \omega_{21}(f) = \frac{\omega_{31}(f)}{2} = \omega_{21}(f), \tag{18}$$

then the second-order susceptibility for the second-harmonic generation can be approximately written as

$$\chi^{(2)}(2\bar{\omega}) = \frac{I_{12}(f)I_{23}(f)I_{31}(f)}{[i\delta(f) + \Gamma_{12}]\Gamma_{13}}. \tag{19}$$

We note that this equation for the second-order susceptibility $\chi^{(2)}(2\bar{\omega})$ is a rough approximation when $\bar{\omega}(f) = \omega_{21}(f)$, i.e., $\delta = 0$. Because the independent-environment assumption for the decays of different energy levels might not always hold and the dissipation rates Γ_{12} and Γ_{13} should be modified. However, the main physics is not changed. In Fig. 3(b), as an example, the amplitude of $\chi^{(2)}(2\bar{\omega})$, which is given by

$$\left|\chi^{(2)}(2\bar{\omega})\right| = \frac{|I_{12}(f)I_{23}(f)I_{31}(f)|}{\Gamma_{13}\sqrt{\delta^2 + \Gamma_{12}^2}}, \tag{20}$$

is plotted as a function of f for given parameters, e.g., $\Gamma_{12}/2\pi = 50$ MHz and $\Gamma_{13}/2\pi = 30$ MHz. It clearly shows that the maximum amplitude of the susceptibility $\chi^{(2)}(2\bar{\omega})$ corresponds to the reduced magnetic flux $f = 0.4878$ or $f = 0.5122$, in which the three energy levels have a harmonic structure. It should be noted that we take Γ_{21} and Γ_{31} as the f-independent parameters for convenience when Fig. 3(b) is plotted. In practice, they should also depend on f.

Measurements

We now take the sum-frequency generation as an example to show how to measure the frequency generation by coupling the three-level SFQC to the continuum of electromagnetic modes confined in a 1D transmission line as for measuring the resonance fluorescence of single artificial atoms[38,39]. As discussed in Ref. 40, if the three transition frequencies of the three-level SFQC are much larger than the decay rates, then we can consider that the decays of different energy levels occur via different dissipation channels. In this case, the inter-

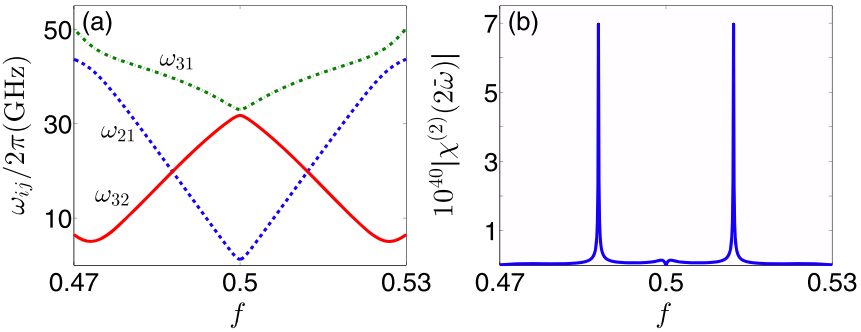

Figure 3 | (a) Three transition frequency ω_{ij} $(i > j)$ versus the reduced magnetic flux f is plotted. The crossing points for the curves of ω_{21} and ω_{32} correspond to $\omega_{21} = \omega_{32}$. (b) The amplitude $\left|\chi^{(2)}(2\bar{\omega})\right|$ of the susceptibility in Eq. (20) versus f is plotted with, e.g., $\Gamma_{21}/2\pi = 50$ MHz and $\Gamma_{31}/2\pi = 30$ MHz. The same SFQC parameters as in Fig. 2 are used in both panels.

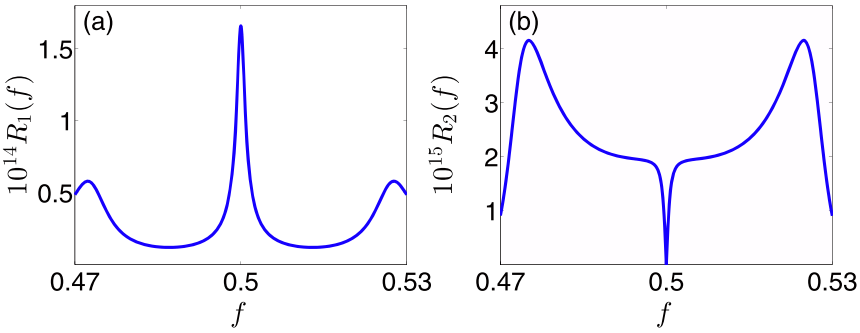

Figure 4 | $R_1(f) \equiv |I_{21}(f)I_{32}(f)|$ and $R_2(f) \equiv |I_{13}(f)I_{32}(f)|$ versus f are plotted in (a) and (b), respectively, for the same SFQC parameters as in Fig. 2.

action Hamiltonian between the three-level SFQC and the continuum modes in the transmission line can be modeled as

$$H_{\rm in} = \int_{-\infty}^{\infty} \frac{d\omega}{\sqrt{2\pi}} \left[\sqrt{\gamma_{12}}a^{\dagger}(\omega)\sigma_{12} + \sqrt{\gamma_{23}}b^{\dagger}(\omega)\sigma_{23} + \sqrt{\gamma_{13}}c^{\dagger}(\omega)\sigma_{13}\right] + \text{H.c.} \quad (21)$$

under the Markovian approximation with the bosonic commutation relation $[\alpha(\omega), \beta^{\dagger}(\omega')] = \delta_{\alpha,\beta}\delta(\omega - \omega')$ with $\alpha, \beta = a, b, c$ for the three kinds of different continuum mode operators. According to the input-output theory[41], the output field centered at the sum-frequency $\omega_1 + \omega_2 = \omega_+$ can be given as

$$\langle c_{\rm out}(t)\rangle = \langle c_{\rm in}(t)\rangle + \sqrt{\gamma_{13}}\,\langle\sigma_{13}(t)\rangle, \quad (22)$$

since $\text{Tr}[\rho\sigma_{13}(t)] = \text{Tr}[\rho(t)\sigma_{13}] = \rho_{31}(t)$. Therefore, up to second order in $V_1(t)$ for the sum-frequency generation, we can approximately obtain the output of the sum-frequency generation as

$$\langle c_{\rm out}(t)\rangle = \frac{\sqrt{\gamma_{13}}}{\hbar^2}\frac{I_{21}(f)I_{32}(f)\Phi(\omega_1)\Phi(\omega_2)\exp(-i\omega_+ t)}{(i\omega_{21} - i\omega_1 + \Gamma_{21})(i\omega_{31} - i\omega_+ + \Gamma_{31})}, \quad (23)$$

where the input field for the continuum mode $c(\omega)$ is in the vacuum. Equation (23) shows that the amplitude of the output field is proportional to the intensities $|\Phi(\omega_1)|$ and $|\Phi(\omega_2)|$ of the two external magnetic fields, the modulus of the product of two transition matrix elements $I_{21}(f)$ and $I_{32}(f)$, and the square root of the decay rate γ_{13}. It is obvious that the intensity of the output field can be tuned by the bias magnetic flux Φ_e. Similarly, the amplitude of the output field for the difference-frequency generation described in Eq. (14) is proportional to the modulus of the product of two transition matrix elements $I_{13}(f)$ and $I_{32}(f)$. The moduli $R_1(f) \equiv |I_{21}(f)I_{32}(f)|$ and $R_2(f) \equiv |I_{13}(f)I_{32}(f)|$ versus f are plotted in Figs. 4(a) and (b), which show that the amplitude of the output fields for the sum- and difference-frequency generations can also be tuned by f. However, the maximum value, corresponding to maximum second-order susceptibility under resonant condition, of $R^{(\max)}(f)$ does not correspond to the maximum value of $R_1(f)$ for the sum-frequency, or $R_2(f)$ for the difference-frequency.

Conclusions

We have proposed and studied a controllable method for generating sum- and difference- frequencies by using three-wave mixing in a single three-level SFQC driven by two weak external fields. Thus, in perturbation theory, the noise and frequency shifts introduced by the driving fields can be neglected and we can obtain all the response functions of different frequencies. We point out that the three-wave-mixing signal can only be generated when the inversion symmetry of the potential energy for the SFQC is broken, that is, the SFQC cannot work at the optimal point. Otherwise, the transition between the ground state and the second-excited state is forbidden, so three-wave mixing cannot be generated as in natural-atom systems. We have shown that the generated microwave signal can be tuned in a very large GHz range. We have also discussed how to generate second-harmonics in the single SFQC. We note that three-wave mixing can also occur in superconducting phase[29–31] and transmon[32] qutrits, when the inversion symmetry of their potential energies is broken. In particular, the phase qutrits might be better for second-harmonic generation because of their small anharmonicity. It should be pointed out that the microwave signal with the sum-frequency might exceed the high-frequency cutoff of the cryogenic amplifier[38]. Thus, the difference-frequency generation should be easier to be experimentally accessed.

In contrast to Ref. 28, with a frequency tunability of about 500 MHz, we show that the tunability of the output frequency using single flux qubit circuits can be a few GHz. Our proposal is valid not only for nondegenerate three-wave mixing, but it can also be applied for second-harmonic generation by changing the bias magnetic flux. Also, contrary to Ref. 28, where the circuit itself is in the classical regime, in our study, the three-wave mixing is generated using excitations of real quantized energy levels of the artificial atoms. Such excitation will result in a strong nonlinearity. Thus, the three-wave mixing in single artificial atoms can be used to generate entangled microwave photons and act as entanglement amplifier or correlated lasing. These could be important toward future quantum networks.

In summary, our study could help generating three- or multi-wave mixing using single artificial atoms. The proposed method is simple and could be used for manipulating second-order and other nonlinear processes in the microwave regime by using single superconducting artificial atoms. Our proposal is realizable using current experimental parameters of superconducting flux qubit circuits.

1. Shen, Y. R. *The Principles of Nonlinear Optics* (Wiley, New York, 2003).
2. Boyd, R. W. *Nonlinear Optics* (Academic Press, New York, 2008).
3. Abrams, R. L., Yariv, A. & Yeh, P. A. Stark-Induced Three-Wave Gases-Part I: Mixing in Molecular Theory. *IEEE J. Quantum Electron.* **QE-13**, 79–82 (1977).
4. Abrams, R. L., Asawa, C. K., Plant, T. K. & Popa, A. E. Stark-Induced Three-Wave Mixing in Molecular Gases-Part II: Experiment. *IEEE J. Quantum Electron.* **QE-13**, 82–85 (1977).
5. Gordy, W. & Cook, R. L. *Microwave Molecular Spectra* (Wiley, New York, 1984).
6. Patterson, D. & Doyle, J. M. Sensitive Chiral Analysis via Microwave Three-Wave Mixing. *Phys. Rev. Lett.* **111**, 023008 (2013).
7. Clarke, J. & Wilhelm, F. K. Superconducting quantum bits. *Nature* **453**, 1031 (2008).
8. Schoelkopf, R. J. & Girvin, S. M. Wiring up quantum systems. *Nature* **451**, 664 (2008).
9. You, J. Q. & Nori, F. Atomic physics and quantum optics using superconducting circuits. *Nature* **474**, 589 (2011).
10. You, J. Q. & Nori, F. Superconducting circuits and quantum information. *Phys. Today* **58** (11), 42 (2005).
11. Buluta, I., Ashhab, S. & Nori, F. Natural and artificial atoms for quantum computation. *Rep. Prog. Phys.* **74**, 104401 (2011).
12. Liu, Y. X., You, J. Q., Wei, L. F., Sun, C. P. & Nori, F. Optical Selection Rules and Phase-Dependent Adiabatic State Control in a Superconducting Quantum Circuit. *Phys. Rev. Lett.* **95**, 087001 (2005).
13. Mooij, J. E. *et al.* Josephson Persistent-Current Qubit. *Science* **285**, 1036 (1999).
14. Deppe, F. *et al.* Two-photon probe of the Jaynes Cummings model and controlled symmetry breaking in circuit QED. *Nature Phys.* **4**, 686 (2008).

15. You, J. Q., Liu, Y. X. & Nori, F. Simultaneous Cooling of an Artificial Atom and Its Neighboring Quantum System. *Phys. Rev. Lett.* **100**, 047001 (2008).
16. You, J. Q., Liu, Y. X., Sun, C. P. & Nori, F. Persistent single-photon production by tunable on-chip micromaser with a superconducting quantum circuit. *Phys. Rev. B* **75**, 104516 (2007).
17. Etaki, S. *et al.* Motion detection of a micromechanical resonator embedded in a d.c. SQUID. *Nature Phys.* **4**, 785 (2008).
18. Doherty, M. W. *et al.* The nitrogen-vacancy colour centre in diamond. *Phys. Rep.* **528**, 1 (2013).
19. Liu, Y. X., Wei, L. F. & Nori, F. Generation of nonclassical photon states using a supercon-ducting qubit in a microcavity. *Europhys. Lett.* **67**, 941 (2004).
20. Houck, A. A. *et al.* Generating single microwave photons in a circuit. *Nature* **449**, 328 (2007).
21. Hofheinz, M. *et al.* Generation of Fock states in a superconducting quantum circuit. *Nature* **454**, 310 (2008).
22. Hofheinz, M. *et al.* Synthesizing arbitrary quantum states in a superconducting resonator. *Nature* **459**, 546 (2009).
23. Eichler, C. *et al.* Observation of Two-Mode Squeezing in the Microwave Frequency Domain. *Phys. Rev. Lett.* **107**, 113601 (2011).
24. Hoi, I. C. *et al.* Generation of Nonclassical Microwave States Using an Artificial Atom in 1D Open Space. *Phys. Rev. Lett.* **108**, 263601 (2012).
25. Rebic, S., Twamley, J. & Milburn, G. J. Giant Kerr Nonlinearities in Circuit Quantum Electrodynamics. *Phys. Rev. Lett.* **103**, 150503 (2009).
26. Hoi, I. C. *et al.* Giant Cross-Kerr Effect for Propagating Microwaves Induced by an Artificial Atom. *Phys. Rev. Lett.* **111**, 053601 (2013).
27. Schackert, F., Roy, A., Hatridge, M., Stone, A. D. & Devoret, M. H. Three-Wave Mixing with Three Incoming Waves: Signal-Idler Coherent Attenuation and Gain Enhancement in a Parametric Amplifier. *Phys. Rev. Lett.* **111**, 073903 (2013).
28. Roch, N. *et al.* Widely Tunable, Nondegenerate Three-Wave Mixing Microwave Device Operating near the Quantum Limit. *Phys. Rev. Lett.* **108**, 147701 (2012).
29. Martinis, J. M., Nam, S., Aumentado, J. & Urbina, C. Rabi Oscillations in a Large Josephson-Junction Qubit. *Phys. Rev. Lett.* **89**, 117901 (2002).
30. Li, J. *et al.* Decoherence, Autler-Townes effect, and dark states in two-tone driving of a three-level superconducting system. *Phys. Rev. B* **84**, 104527 (2011).
31. Li, J. *et al.* Dynamical Autler-Townes control of a phase qubit. *Sci. Rep.* **2**, 645 (2012).
32. Houck, A. A. *et al.* Controlling the Spontaneous Emission of a Superconducting Transmon Qubit. *Phys. Rev. Lett.* **101**, 080502 (2008).
33. Liu, Y. X., Yang, C. X., Sun, H. C. & Wang, X. B. Coexistence of single- and multi-photon processes due to longitudinal couplings between superconducting flux qubits and external fields. *New J. Phys.* **16**, 015031 (2014).
34. Liu, Y. X., Wei, L. F., Tsai, J. S. & Nori, F. Controllable Coupling between Flux Qubits. *Phys. Rev. Lett.* **96**, 067003 (2006).
35. Liu, Y. X., Wei, L. F., Johansson, J. R., Tsai, J. S. & Nori, F. Superconducting qubits can be coupled and addressed as trapped ions. *Phys. Rev. B* **76**, 144518 (2007).
36. Harrabi, K., Yoshihara, F., Niskanen, A. O., Nakamura, Y. & Tsai, J. S. Engineered selection rules for tunable coupling in a superconducting quantum circuit. *Phys. Rev. B* **79**, 020507(R) (2009).
37. Ashhab, S. *et al.* Interqubit coupling mediated by a high-excitation-energy quantum object. *Phys. Rev. B* **77**, 014510 (2008).
38. Astafiev, O. *et al.* Resonance Fluorescence of a Single Artificial Atom. *Science* **327**, 840 (2010).
39. Zhou, L., Gong, Z. R., Liu, Y. X., Sun, C. P. & Nori, F. Controllable Scattering of a Single Photon inside a One-Dimensional Resonator Waveguide. *Phys. Rev. Lett.* **101**, 100501 (2008).
40. Joo, J., Bourassa, J., Blais, A. & Sanders, B. C. Electromagnetically Induced Transparency with Amplification in Superconducting Circuits. *Phys. Rev. Lett.* **105**, 073601 (2010).
41. Walls, D. F. & Milburn, G. J. *Quantum Optics* (Springer, Berlin, 2008).

Acknowledgments

Y.X.L. is supported by the National Basic Research Program of China Grant No. 2014CB921401, the NSFC Grants No. 61025022, and No. 91321208. A.M. is supported by Grant No. DEC-2011/03/B/ST2/01903 of the Polish National Science Centre. F.N. is partially supported by the RIKEN iTHES Project, MURI Center for Dynamic Magneto-Optics, and a Grant-in-Aid for Scientific Research (S). Z.H.P. and J.S.T. were supported by Funding Program for World-Leading Innovative R & D on Science and Technology (FIRST), MEXT KAKENHI "Quantum Cybernetics".

Author contributions

Y.X.L. proposed the main idea. Y.X.L., H.C.S., Z.H.P., A.M. and F.N. contributed to the findings of this work and wrote the manuscript. J.S.T. participated in the discussions.

Additional information

Competing financial interests: The authors declare no competing financial interests.

How to cite this article: Liu, Y. *et al.* Controllable microwave three-wave mixing via a single three-level superconducting quantum circuit. *Sci. Rep.* **4**, 7289; DOI:10.1038/srep07289 (2014).